The Astrophysical Journal, 649:243–247, 2006 September 20

AN EMPIRICAL TOOL TO DERIVE METALLICITY, REDDENING, AND DISTANCE FOR OLD STELLAR POPULATIONS FROM NEAR-INFRARED COLOR-MAGNITUDE DIAGRAMS [1]

Francesco R. Ferraro,[2] Elena Valenti,[2,3] and Livia Origlia[3]

Received 2006 February 8; accepted 2006 May 18

ABSTRACT

We present an empirical method to derive photometric metallicity, reddening, and distance to old stellar populations by using a few major features of the red giant branch (RGB) in near-IR color-magnitude diagrams. We combine the observed RGB features with a set of equations linking the global metallicity [M/H] to suitable RGB parameters (colors, magnitudes, and slope), as calibrated from a homogeneous sample of Galactic globular clusters with different metallicities. This technique can be applied to efficiently derive the main population parameters of old stellar systems, with the goal of using ground-based adaptive optics and space facilities to probe the stellar content of remote galaxies.

Subject headings: Galaxy: evolution — Galaxy: fundamental parameters — globular clusters: general — infrared: stars — stars: Population II — techniques: photometric

1. INTRODUCTION

Stellar populations are fundamental tracers of the formation and evolution history of their parent galaxies. The accurate determination of their basic parameters (such as age, metallicity, and distance) is then crucial, but the ability to do so is restricted to a number of relatively nearby stellar systems, for which single stars are spatially resolved and whose magnitudes can be accurately determined. At least the brightest portion of the red giant branch (RGB) is needed in order to have hits on metallicity and distance, while the detection of the main sequence turnoff (MS-TO) is required to get the age. In this respect, detailed investigations of simple stellar populations (SSPs, i.e., coeval and chemically homogeneous stellar aggregates) offer a unique opportunity to empirically calibrate suitable photometric indices and evolutionary features in terms of the overall metallicity of the system.

Stellar clusters represent the best known approximation of SSPs in the universe, hence they are ideal tools for this purpose. An empirical method to simultaneously find metallicity and reddening from the morphology and location of the RGB in the (I, $V-I$) color-magnitude diagram (CMD) was presented a decade ago (Sarajedini 1994). More recently, this method has been extended to the (V, $B-V$) plane by Sarajedini & Layden (1997), and further improved by Carretta & Bragaglia (1998) and Ferraro et al. (1999) by adopting the Carretta & Gratton (1997) and the global ([M/H]) metallicity scale, respectively. The method presented here adopts the most recent calibrations, as obtained from a large IR photometric database of globular clusters (GCs), collected by our group with different instruments at the ESO telescopes (La Silla, Chile) and at the TNG (Italian Telescopio Nazionale Galileo; La Palma, Spain) over the last decade in the framework of a long-term project devoted to study the photometric properties of the RGB (Ferraro et al. 1994, 1995, 2000; Montegriffo et al. 1995; Sollima et al. 2004; Valenti et al. 2004a, 2004b, 2004c). In particular, we have recently presented a complete set of photometric indices (colors, magnitudes, and slopes) describing the location and morphology of the RGB and calibrations in terms of the global cluster metallicity (Valenti et al. 2004a), together with the empirical calibrations of the IR luminosity of the two major RGB evolutionary features, namely the RGB bump and tip (Valenti et al. 2004b). It is worth mentioning that the calibration relations used in this study rely on a database whose properties have been derived in a fully self-consistent way. In fact, the adopted estimates of the cluster reddening, metallicity, and distance are based (1) on a homogeneous photometric system; (2) on the Ferraro et al. (1999) distance scale, which relies on the most recent and largest database of Galactic GCs; and (3) on a uniform and high-resolution metallicity scale (Carretta & Gratton 1997).

The calibration of suitable relations to derive metallicity, reddening, and distance in the near-IR plane is crucial in the study of extragalactic bulges, which can be characterized by high metallicities and can be affected by severe reddening. The current generation of ground-based IR instrumentation with high resolution and wide-field coverage, and the future availability of the *James Webb Space Telescope* will allow us to resolve the brightest giants in galaxies up to several Mpc away, and to derive their overall metallicity, reddening, and distance modulus with great accuracy.

The paper is organized as follows. Section 2 discusses the adopted metallicity scale, while §§ 3.1 and 3.2 present the equation sets for both the disklike and bulgelike enrichment scenarios , respectively. Section 4 describes the computational routine that provides photometric estimates of metallicity, reddening, and distance, while in § 5 we test the described method on two template GCs in the Galactic bulge and in the Large Magellanic Cloud, namely NGC 6539 and NGC 1978, respectively, in order to demonstrate its reliability.

2. THE GLOBAL METALLICITY

As extensively discussed in Ferraro et al. (1999, 2000), a correct parameterization of the RGB characteristics as a function of the metal content of the population does require knowledge of the so-called "global" metallicity, which takes into account the iron as well as the α-element abundances. This is an important point, since the location of the RGB strongly depends on the low ionization potential [Fe+Mg+Si/H] abundance mixture (Straniero & Chieffi 1991; Salaris & Cassisi 1996) rather than on [Fe/H] abundance alone. In fact, low ionization potential elements are the main contributors to free electrons, which generate the H^- ion,

[1] Based on observations collected at the European Southern Observatory (ESO), La Silla, Chile. Also based on observations made with the Italian Telescopio Nazionale Galileo (TNG), operated on the island La Palma by the Fundacion Galileo Galilei of INAF (Istituto Nazionale di Astrofisica) at the Spanish Observatorio del Roque de los Muchachos of the Instituto de Astrofisica de Canarias.

[2] Dipartimento di Astronomia Università di Bologna, via Ranzani 1, I-40127 Bologna, Italy; francesco.ferraro3@unibo.it, elena.valenti3@unibo.it.

[3] INAF-Osservatorio Astronomico di Bologna, via Ranzani 1, I-40127 Bologna, Italy; livia.origlia@bo.astro.it.

the major component responsible for the continuum opacity in the RGB temperature range (3000–6000 K; Renzini 1977).

In halo/disk field stars, the average [α/Fe] abundance ratio shows a general enhancement of 0.3–0.5 dex with respect to the solar value up to [Fe/H] ≈ -1 (see, e.g., Boesgaard et al. 1999; Gratton et al. 2000; Carretta et al. 2000, and references therein) and a linear decreasing trend toward solar [α/Fe] with further increasing metallicity. An [α/Fe] enhancement is also found in the metal-poor halo GCs (see, e.g., Gratton et al. 2004; Sneden et al. 2004, and references therein). However, until a few years ago, only a few measurements were available in the high-metallicity regime to properly define the [α/Fe] trend in GCs (see, e.g., Kraft 1994; Carney 1996). The actual position of the knee (i.e., the metallicity at which [α/Fe] begins to decrease) depends on the Type Ia supernova (SN) timescales, and it is also a function of the star formation rate, while the amount of α-enhancement depends on the initial mass function of the progenitors of the Type II SNe (see McWilliam 1997).

Measurements of metal-rich field and cluster giants toward the Galactic bulge are a recent accomplishment of high-resolution optical and IR spectroscopy. Bulge stars are indeed ideal targets to study the behavior of the abundance patterns in the high-metallicity domain, but foreground extinction is so great as to largely preclude optical studies of any kind, particularly at high spectral resolution. The most accurate abundance determinations obtained so far based on high-resolution optical spectroscopy refer to a sample of K giants in Baade's window (McWilliam & Rich 1994; Rich & McWilliam 2000; Fulbright et al. 2004) and a few giants in two GCs, namely NGC 6553 and NGC 6528 (Carretta et al. 2001; Zoccali et al. 2004). Recently, high-resolution IR spectroscopic measurements of M giants in Baade's window (Rich & Origlia 2005), as well as bulge GCs (Origlia et al. 2002; Meléndez et al. 2003; Origlia & Rich 2004; Lee et al. 2004; Origlia et al. 2005a, 2005b) dramatically extended the sample of measured bulge stars. All these studies point toward a α-enhancement by a factor of 2–3 up to solar metallicity.

3. THE ADOPTED ENRICHMENT SCENARIOS

In the computation of the global metallicity for a sample of 61 Galactic globular clusters (GGCs), Ferraro et al. (1999) used a constant [α/Fe] = 0.28 for [Fe/H] < -1 and linearly decreasing to zero at $-1 <$ [Fe/H] < 0. In the following, we compute two independent sets of global metallicities and photometric relations, according to two different scenarios (see Fig. 1):

Scenario (1): Disklike enhancement (according to Ferraro et al. 1999) [α/Fe] = 0.3 for [Fe/H] < -1, and [α/Fe] linearly decreasing to zero for $-1 <$ [Fe/H] ≤ 0.

Scenario (2): Bulgelike enhancement (according to Carney's [1996] suggestions and the recent results on the bulge field and cluster populations) [α/Fe] = 0.30 constant over the entire range of metallicity ($-2 \leq$ [Fe/H] ≤ 0).

The set of equations discussed in Valenti et al. (2004a, hereafter Paper I) and Valenti et al. (2004b, hereafter Paper II) have been computed according to scenario (1). Here we present similar equations for scenario (2), so the reader can choose the equation set that turns out to be the most suitable to the describe the stellar system.

In both scenarios, the contribution of the α-element enhancement has been taken into account by simply rescaling standard models to the global metallicity [M/H] according to the relation (Salaris et al. 1993)

$$[\mathrm{M/H}] = [\mathrm{Fe/H}] + \log(0.638 f_\alpha + 0.362), \quad (1)$$

where f_α is the enhanced factor of the α-elements.

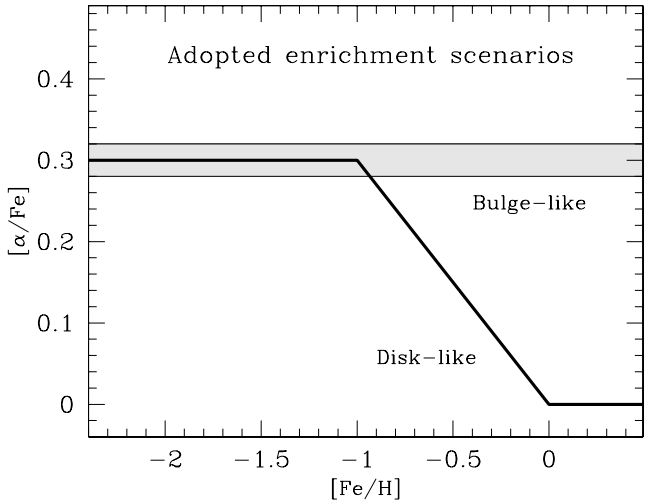

FIG. 1.—Sketched diagram of the [α/Fe] vs. [Fe/H] trend in the disk-/bulge-like enrichment scenarios, as adopted in our computational routine.

3.1. *The Equation Set in the Disklike Enrichment Scenario*

In this section, we present and discuss the equation set adopted to construct the computational routine that provides metallicity, reddening, and distance of a stellar population, by using the RGB observables in the (M_K, $J-K$) IR plane. Note that the validity of the relations has been extended up to [M/H] $\sim +0.4$ dex with respect to the results presented in Paper I, including the recent results on the metallicity of NGC 6791 (Origlia et al. 2006). Hence the relations presented here have been obtained in the metallicity range: $-2.16 \leq$ [Fe/H] $\leq +0.4$ dex.[4]

The overall metallicity of a stellar population can be linked to the slope of the RGB (slope$_{\mathrm{RGB}}$) as defined in the near-IR CMD by Kuchinski et al. (1995) and Kuchinski & Frogel (1995), according to the relation

$$[\mathrm{M/H}] = -2.53 - 20.83(\mathrm{slope}^{JK}_{\mathrm{RGB}}), \quad (2.1)$$

where slope$^{JK}_{\mathrm{RGB}}$ is the RGB slope measured following the prescriptions discussed in Paper I in the (M_K, $J-K$) CMD.

The RGB-tip luminosity is a quantity predicted well by theoretical models, and it can be easily measured in populous stellar systems like galaxies. The luminosity of the RGB tip for stellar populations older than $t \sim$ 1–2 Gyr is nearly independent from the population age. Moreover, it turns out to be particularly bright in the near-IR ($M_K \sim -6$); hence it is a very promising standard candle up to large distances. The main limitation of this method is the clear-cut determination of the RGB-tip luminosity, which could be seriously affected by low-number statistics. In fact, the rapid star evolution near the end of the RGB makes the brightest portion of the RGB intrinsically poorly populated. However, this problem is marginal in very populous stellar systems. The dependence of this feature on the overall metallicity of the stellar population has been empirically determined by using a sample of Galactic GCs (see Paper II), and it turns out to be in good agreement with theoretical expectations. Here we report the relation obtained in Paper II:

$$M_K^{\mathrm{tip}} = -6.92 - 0.62[\mathrm{M/H}]. \quad (2.2)$$

[4] Note that the inclusion of NGC 6791 in our calibrator clusters sample does not significantly change the relation derived in Paper I.

As is well known (see Salaris & Girardi 2002; Grocholski & Sarajedini 2002), for clusters older than 2 Gyr, the level of the helium-burning red clump (RC) is mainly influenced by metallicity, and shows little dependence on its age. Hence, for relatively old metal-rich populations ($t > 2$ Gyr, $[\mathrm{M/H}] > -1$), it is also possible to use the level of the RC as an additional distance indicator. We estimate the mean level of the RC by using a metal-rich ($-0.9 < [\mathrm{Fe/H}] < -0.3$) cluster subsample (namely, 47 Tuc, NGC 6342, NGC 6380, NGC 6441, NGC 6440, NGC 6553, NGC 6528, and NGC 6637) selected from the global database presented in Paper I. The value turns out to be:

$$M_K^{\mathrm{RC}} = -1.40 \pm 0.2. \tag{2.3}$$

Note that most selected clusters can be considered coeval within 10%–20% according to De Angeli et al. (2005), who measured the relative ages of 47 Tuc, NGC 6342, NGC 6637, and Ortolani et al. (1995, 2001), who measured the relative ages of 47 Tuc, NGC 6528, and NGC 6553. The adopted uncertainty of ± 0.2 in equation (2.2) takes into account the metallicity dependence of the RC position on the metallicity range spanned by our metal-rich GC subsample ($\delta[\mathrm{Fe/H}] \sim 0.6$ dex). In fact, according to Table 1 by Salaris & Girardi (2002), the M_K^{RC} level is expected to vary ~ 0.15 mag at $t = 10$ Gyr over such a metallicity range. Moreover, in the age range 2–10 Gyr, at fixed metallicity ($[\mathrm{M/H}] = -0.68$), the M_K^{RC} varies 0.03 mag per Gyr. Hence the 0.2 mag uncertainty adopted as conservative estimate of the M_K^{RC} level is expected to be reasonable over the considered range of age and metallicity.

The absolute magnitude of the RGB at fixed color is another observable that can be used to define useful relations with the overall metallicity. Here we report the calibrations discussed in Paper I:

$$M_K^{(J-K)_0=0.7} = -1.38 + 2.22[\mathrm{M/H}]. \tag{2.4}$$

Finally, the entire set of equations describing the RGB location in (J–K) color at different levels of magnitude ($M_K = -5.5, -5, -4, -3$) are listed:

$$[\mathrm{M/H}] = -4.37 + 3.84(J-K)_0^{-5.5}, \tag{2.5}$$

$$[\mathrm{M/H}] = -4.51 + 4.24(J-K)_0^{-5}, \tag{2.6}$$

$$[\mathrm{M/H}] = -4.87 + 5.20(J-K)_0^{-4}, \text{ and} \tag{2.7}$$

$$[\mathrm{M/H}] = -5.36 + 6.48(J-K)_0^{-3}. \tag{2.8}$$

3.2. *The Equation Set in the Bulge-Like Enrichment Scenario*

An analogous set of eight equations can be obtained in the *bulgelike* enrichment scenario. Here we list the complete equation set, based on the database presented in Paper I and Paper II, by adopting a constant $[\alpha/\mathrm{Fe}]$ over the entire range of metallicity:

$$[\mathrm{M/H}] = -2.63 - 22.50(\mathrm{slope}_{\mathrm{RGB}}^{JK}), \tag{3.1}$$

$$M_K^{\mathrm{tip}} = -6.84 - 0.56[\mathrm{M/H}], \tag{3.2}$$

$$M_K^{\mathrm{RC}} = -1.40 \pm 0.2, \tag{3.3}$$

$$M_K^{(J-K)_0=0.7} = -1.58 + 2.08[\mathrm{M/H}], \tag{3.4}$$

$$[\mathrm{M/H}] = -4.59 + 4.13(J-K)_0^{-5.5}, \tag{3.5}$$

$$[\mathrm{M/H}] = -4.74 + 4.55(J-K)_0^{-5}, \tag{3.6}$$

$$[\mathrm{M/H}] = -5.12 + 5.58(J-K)_0^{-4}, \text{ and} \tag{3.7}$$

$$[\mathrm{M/H}] = -5.64 + 6.94(J-K)_0^{-3}. \tag{3.8}$$

4. THE COMPUTATIONAL ROUTINE

The computational routine requires as input parameters:

1. The observed RGB mean ridge line in the (K, $J-K$) CMD;
2. The observed RGB slope ($\mathrm{slope}_{\mathrm{RGB}}^{JK}$); and
3. The observed RGB-Tip ($K_{\mathrm{tip}}^{\mathrm{obs}}$) and/or the RC level ($K_{\mathrm{RC}}^{\mathrm{obs}}$).

Figure 2 shows the flow diagram of the computational routine. In the following, we refer to either equations (2.1)–(2.8) or (3.1)–(3.8), depending on the adopted enrichment scenario.

Since the RGB slope is independent of the cluster distance and reddening, we can use equation (2.1) or (3.1) to get a first guess of the population metallicity. By using this first-guess metallicity, it is possible to derive the expected level of the RGB tip from equation (2.2) or (3.2). Hence, the comparison with the observed value ($K_{\mathrm{tip}}^{\mathrm{obs}}$) will directly yield the first estimate of the distance modulus $(m-M)_K$. For the (closest) metal-rich stellar systems for which the RC is observed, an independent estimate of the modulus can be also derived from the comparison with the mean RC levels reported in equation (2.3) and (3.3).

By using the first-guess metallicity and equation (2.4) or (3.4) it is also possible to obtain the expected absolute magnitude (M_K^{exp}) at fixed color $[(J-K)_0 = 0.7]$.

Now the mean ridge line of the program population can be corrected by using the distance modulus obtained above; the observed color $[(J-K)^{\mathrm{obs}}]$ in correspondence of the derived magnitude (M_K^{exp}) will yield the first-guess estimate of the reddening,

$$E(B-V) = \left[(J-K)^{\mathrm{obs}} - 0.7\right]/(0.87 - 0.38),$$

where the extinction coefficients from Savage & Mathis (1979) have been adopted.

The color of the input RGB mean ridge line can be now dereddened and transformed into the absolute plane $[M_K, (J-K)_0]$. Once in the absolute plane, the color at fixed magnitude levels can be measured and inserted in equations (2.5)–(2.8) or equations (3.5)–(3.8) to get a new mean value of metallicity. The latter can be inserted in equation (2.2) or (3.2), and the overall procedure iterated until the values of the three output quantities, namely metallicity, reddening, and distance, converge within suitable ranges, which can be specified as input tolerances.

The formal error on each derived quantity can be estimated by using a simple Monte Carlo simulation. In doing this, we randomly extracted a large number of values for each of the three main observables (namely $\mathrm{slope}_{\mathrm{RGB}}^{JK}$, $K_{\mathrm{obs}}^{\mathrm{tip}}$, and $K_{\mathrm{RC}}^{\mathrm{obs}}$) from a Gaussian distribution peaked on the observed value, with σ equal to the uncertainty of each observable. These values are used (following the scheme plotted in Fig. 2) to derive metallicity, reddening, and distance. The standard deviation of each set of values is the error associated to that specific quantity. However, beside the formal errors obtained from this procedure [typically $\delta(m-M)_0 = \pm 0.10 - 0.15$ mag, $\delta E(B-V) = \pm 0.03 - 0.04$ mag, and $\delta[\mathrm{M/H}] = \pm 0.10 - 0.15$ dex] we estimate that conservative uncertainties for the derived quantities are $\delta(m-M)_0 = \pm 0.2$ mag, $\delta E(B-V) = \pm 0.05$ mag, and $\delta[\mathrm{M/H}] = \pm 0.2$ dex.

5. TEST CASES: NGC 1978 AND NGC 6539

To test the reliability of the proposed technique, we have chosen two metal-rich clusters for which accurate determination

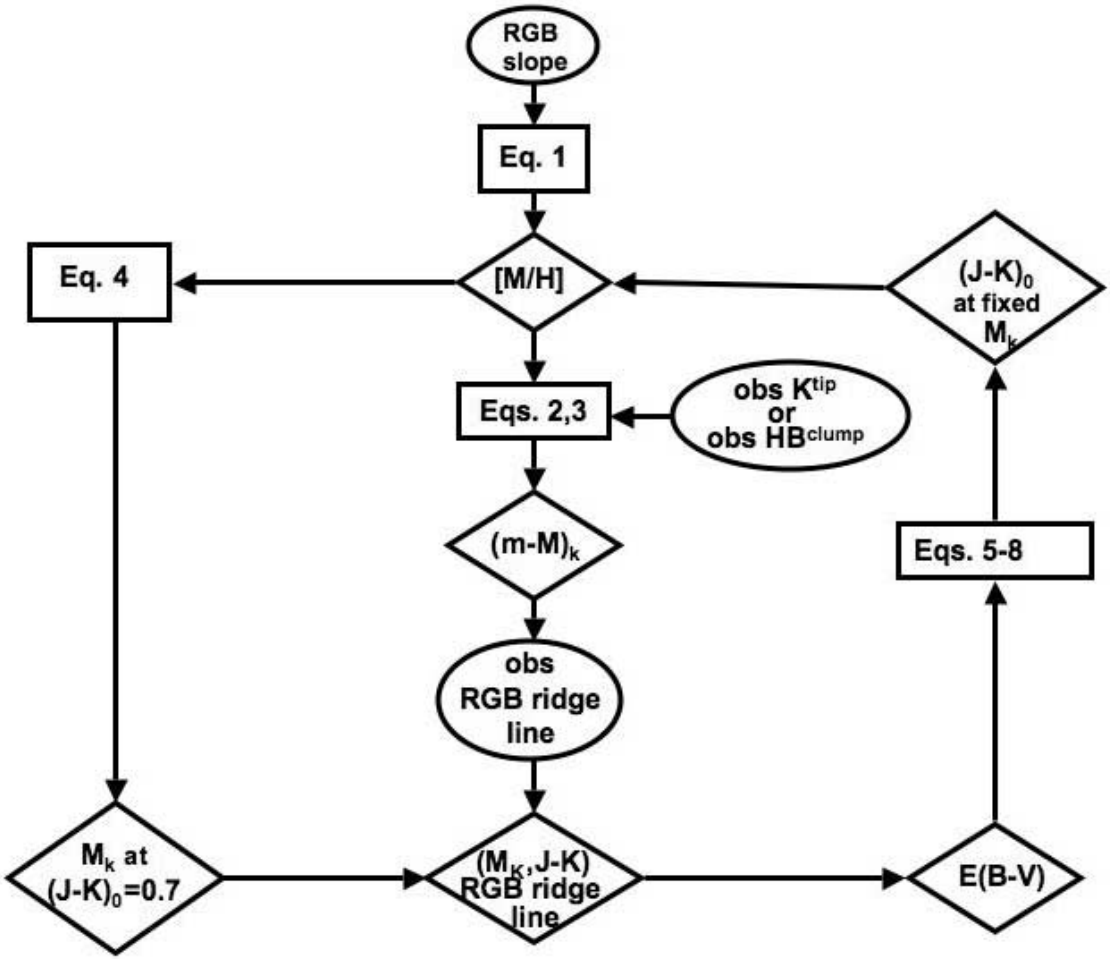

FIG. 2.—Flow diagram of the computational routine used to simultaneously derive distance, reddening, and metallicity of an old stellar population from the RGB morphology (slope, colors, luminosity) and evolutionary features (RGB-tip and red clump) in the near IR CMDs.

of the metallicity have been recently obtained: the Large Magellanic Cloud cluster NGC 1978, and the Galactic bulge cluster NGC 6539. The CMDs of NGC 1978 and NGC 6539 reported in Figures 3 and 4 are from Mucciarelli et al. (2006) and from Origlia et al. (2005b), respectively. The RGB mean ridge lines, computed following the prescriptions described in Paper I, are also overplotted as solid lines on the CMDs of Figures 3 and 4.

In the case of NGC 1978, the CMD shown in Figure 3 has been used to measure the RGB slope ($\mathrm{slope}^{JK}_{\mathrm{RGB}} = -0.104$) and to estimate the observed RGB-tip ($K^{\mathrm{obs}}_{\mathrm{tip}} = 11.89$). It is worth noticing that this cluster is suspected to be a relatively young cluster ($t \sim 2$ Gyr), hence we do not use its RC level in deriving the distance modulus,[5] since for extremely young clusters, the $K^{\mathrm{obs}}_{\mathrm{RC}}$ level is a sensible function of the age of the population (see, e.g., Fig. 3 and Table 1 of Salaris & Girardi 2002).

By running the computational routine with the input parameters quoted above, a good convergence is reached after few iterations. In the bulgelike scenario, the computational routine leaded a reddening estimate of $E(B-V) = 0.09 \pm 0.04$ mag, an intrinsic distance modulus of $(m-M)_0 = 18.53 \pm 0.18$ mag and a metallicity of $[\mathrm{M/H}] = -0.29 \pm 0.14$ dex. In the disklike scenario the following solutions have been obtained: $E(B-V) = 0.09 \pm 0.04$ mag, $(m-M)_0 = 18.55 \pm 0.19$ mag, and $[\mathrm{M/H}] = -0.36 \pm 0.12$ dex. These values are fully consistent with the results found

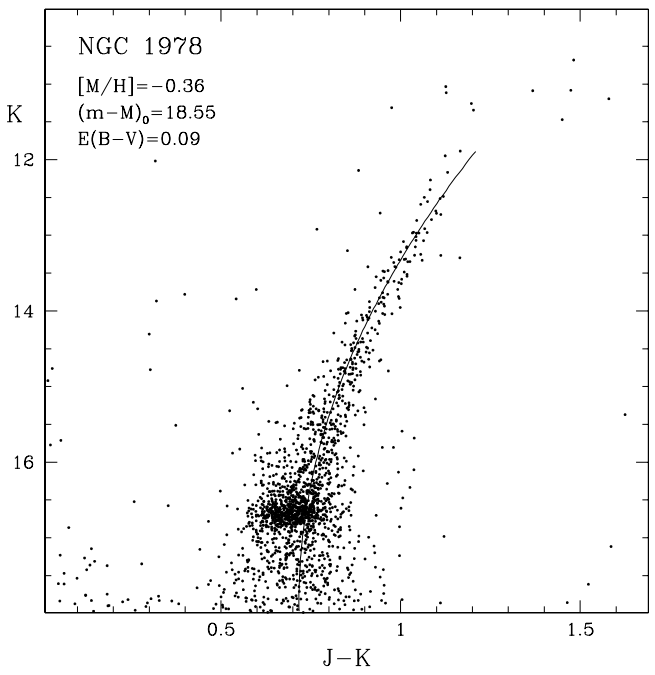

FIG. 3.—Observed K, $(J-K)$ color-magnitude diagram of NGC 1978. The derived RGB fiducial ridge line is overplotted as a solid line. The derived metallicity, distance, and reddening solutions within the disklike scenario are also shown.

[5] Only the $K^{\mathrm{tip}}_{\mathrm{obs}}$ level has been used for this cluster.

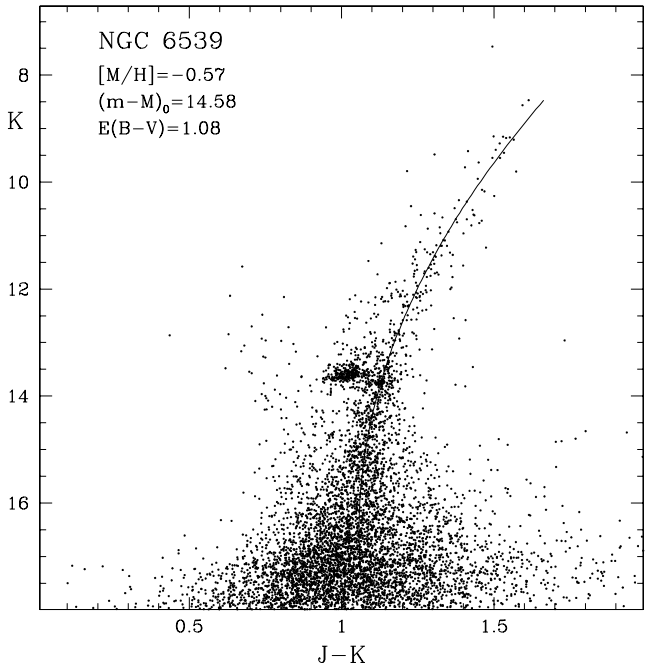

FIG. 4.—Observed K, $(J-K)$ color-magnitude diagram of NGC 6539. The derived RGB fiducial ridge lines are overplotted as a solid line. The derived metallicity, distance, and reddening solutions within the bulgelike scenario are also shown.

by Persson et al. (1983) and Schlegel et al. (1998) for the extinction [$E(B-V)=0.100$, and $E(B-V)=0.075$, respectively], by Van Den Bergh (1998) and Alves (2004) for the distance [$(m-M)_0=18.48$ and $(m-M)_0=18.50$, respectively], and by Ferraro et al. (2006) and Olszewski et al. (1991) for the metallicity ([Fe/H] $=-0.38$ dex and [Fe/H] $=-0.42$ dex, based on high-resolution optical spectra and on the calcium triplet, respectively).

Adopting the same strategy followed in the case of NGC 1978, we have analyzed the CMD of NGC 6539 (Origlia et al. 2005b), finding a slope$^{JK}_{\rm RGB}=-0.091$ and $K^{\rm obs}_{\rm tip}=8.47$ mag. From the derived K luminosity function, we also estimated the RC level to be $K^{\rm obs}_{\rm RC}=13.60$ mag. By running the computational routine within the bulgelike scenario, we found a reddening of $E(B-V)=1.08\pm0.06$ mag, an intrinsic distance modulus of $(m-M)_0=14.58\pm0.15$ mag, and a global metallicity [M/H] $=-0.57\pm0.15$ dex. The derived metallicity is fully consistent within 0.2 dex with the recent estimate, based on high-resolution ($R\approx25000$) IR spectroscopy, by Origlia et al. (2005b), who found [Fe/H] $=-0.76$ dex. The obtained reddening value is also in excellent agreement with the estimate listed in the Harris (1996)[6] compilation [$E(B-V)=1.00$], and with the Schlegel et al. (1998) extinction map [$E(B-V)=1.09$]. Our distance value turns out to be 0.1 mag larger than the Harris (1996) estimate.[7]

This research is supported by the Agenzia Spaziale Italiana (ASI) and the Ministero dell'Istruzione, dell'Università e della Ricerca. We thank the anonymous referee for his/her helpful comments and suggestions, which significantly contributed to improve the paper presentation.

[6] For the 2003 updated version, see http://physwww.mcmaster.ca/%7Eharris/mwgc.dat.

[7] Note that the adopted calibrations are based on the Ferraro et al. (1999) distance scale, which is ≈0.15–0.20 mag longer than the one by Harris (1996).

REFERENCES

Alves, D. R. 2004, NewA Rev., 48, 659
Boesgaard, A. M., King, J. R., Deliyannis, C. P., & Vogt, S. S. 1999, AJ, 117, 492
Carney, B. W. 1996, PASP, 108, 900
Carretta, E., & Bragaglia, A. 1998, A&A, 329, 937
Carretta, E., Cohen, J., Gratton, R. G., & Behr, B. 2001, AJ, 122, 1469
Carretta, E., & Gratton, R. G. 1997, A&AS, 121, 95
Carretta, E., Gratton, R. G., & Sneden, C. 2000, A&A, 356, 238
De Angeli, F., Giampaolo, P., Santi, C., Giorgia, B., Alejandra, R.-B., Maurizio, S., Antonio, A., & Alfred, R. 2005, AJ, 130, 116
Ferraro, F. R., Fusi Pecci, F., Guarnieri, M. D., Moneti, A., Origlia, L., & Testa, V. 1994, MNRAS, 266, 829
Ferraro, F. R., Fusi Pecci, F., Montegriffo, P., Origlia, L., & Testa, V. 1995, A&A, 298, 461
Ferraro, F. R., Messineo, M., Fusi Pecci, F., De Palo, M. A., Straniero, O., Chieffi, A., & Limongi, M. 1999, AJ, 118, 1738
Ferraro, F. R., Montegriffo, P., Origlia, L., Fusi Pecci, F. 2000, AJ, 119, 1282
Ferraro, F. R., Mucciarelli, A., Carretta, E., & Origlia, L. 2006, ApJ, 645, L33
Fulbright, J. P., Rich, R. M., & McWilliam, A. 2004, AAS, 205, 7706
Gratton, R. G., Sneden, C., & Carretta, E. 2004, ARA&A, 42, 385
Gratton, R. G., Sneden, C., Carretta, E., & Bragaglia, A. 2000, A&A, 354, 169
Grocholski, A. J., & Sarajedini, A. 2002, AJ, 123, 1603
Harris, W. E. 1996, AJ, 112, 1487
Kraft, R. P. 1994, PASP, 106, 553
Kuchinski, L. E., & Frogel, J. A. 1995, AJ, 110, 2844
Kuchinski, L. E., Frogel, J. A., Terndrup, D. M., & Persson, S. E. 1995, AJ, 109, 1131
Lee, J., Carney, B. W., & Balachandran, S. C. 2004, AJ, 128, 2388
McWilliam, A. 1997, ARA&A, 35, 503
McWilliam, A., & Rich, R. M. 1994, ApJS, 91, 749
Meléndez, J., Barbuy, B., Bica, E., Zoccali, M., Ortolani, S., Renzini, A., & Hill, V. 2003, A&A, 411, 417
Montegriffo, P., Ferraro, F. R., Fusi Pecci, F., & Origlia, L. 1995, MNRAS, 276, 739
Mucciarelli, A., Origlia, L., Ferraro, F. R., Maraston, C., & Testa, V. 2006, ApJ, 646, 939, in press
Olszewski, E. W., Schommer, R. A., Suntzeff, N. B., & Harris, H. C. 1991, AJ, 101, 515
Origlia, L., & Rich, R. M. 2004, AJ, 127, 3422
Origlia, L., Rich, R. M., & Castro, S. 2002, AJ, 123, 1559
Origlia, L., Valenti, E., & Rich, R. M. 2005a, MNRAS, 356, 1276
Origlia, L., Valenti, E., Rich, R. M., & Ferraro, F. R 2005b, MNRAS, 363, 897
———. 2006, MNRAS, in press (astro-ph/0604030)
Ortolani, S., Barbuy, B., Bica, E., Renzini, A., Zoccali, M., Rich, R. M., & Cassisi, S. 2001, A&A, 376, 878
Ortolani, S., Renzini, A., Gilmozzi, R., Marconi, G., Barbuy, B., Bica, E., & Rich, R. M. 1995, Nature, 337, 701
Persson, S. E., Aaronson, M., Cohen, J. G., Frogel, J. A., & Matthews, K. 1983, ApJ, 266, 105
Renzini, A. 1977, in Advanced Stages in Stellar Evolution, ed. P. Bouvier & A. Maeder (Sauverny: Obs. Geneva), 151
Rich, R. M., & McWilliam, A. 2000, Proc. SPIE, ed. J. Bergeron, 4005, 150
Rich, R. M., & Origlia, L. 2005, ApJ, 634, 1293
Salaris, M., & Cassisi, S. 1996, A&A, 305, 858
Salaris, M., Chieffi, A., & Straniero, O. 1993, ApJ, 414, 580
Salaris, M., & Girardi, L. 2002, MNRAS, 337, 332
Sarajedini, A. 1994, AJ, 107, 618
Sarajedini, A., & Layden, A. 1997, AJ, 113, 264
Savage, B. D., & Mathis, J. S. 1979, ARA&A, 17, 73
Schlegel, D. J., Finkbeiner, D. P., & Davis, M. 1998, ApJ, 500, 525
Sneden, C., Kraft, R. P., Guhathakurta, P., Peterson, R. C., Fulbright, J. P. 2004, AJ, 127, 2162
Sollima, A., Ferraro, F. R., Origlia, L., Pancino, E., & Bellazzini, M. 2004, A&A, 420, 173
Straniero, O., & Chieffi, A. 1991, ApJS, 76, 525
Valenti, E., Ferraro, F. R., & Origlia, L. 2004a, MNRAS, 351, 1204, Paper I
———. 2004b, MNRAS, 354, 815, Paper II
Valenti, E., Ferraro, F. R., Perina, S., & Origlia, L. 2004c, A&A, 419, 139
Van Den Bergh, S. 1998, PASP, 110, 1377
Zocali, M. et al. 2004, A&A, 423, 507